ORIGINAL ARTICLE doi: 10.2176/jns-nmc.2022-0010

*Neurol Med Chir (Tokyo) 62, 361-368, 2022* Online May 25, 2022

# *Primary Experiences with Robot-assisted Navigation-based Frameless Stereo-electroencephalography: Higher Accuracy than Neuronavigation-guided Manual Adjustment*

Yuichiro KOJIMA,[1] Takehiro UDA,[1,2] Toshiyuki KAWASHIMA,[1] Saya KOH,[1] Masato HATTORI,[1] Yuki MITO,[1] Noritsugu KUNIHIRO,[2] Shohei IKEDA,[2] Ryoko UMABA,[2] and Takeo GOTO[1]

[1]*Department of Neurosurgery, Osaka Metropolitan University Graduate School of Medicine, Osaka, Osaka, Japan*
[2]*Department of Pediatric Neurosurgery, Osaka City General Hospital, Osaka, Osaka, Japan*

## Abstract

**The use of robot-assisted frameless stereotactic electroencephalography (SEEG) is becoming more common. Among available robotic arms, Stealth Autoguide (SA) (Medtronic, Minneapolis, MN, USA) functions as an optional instrument of the neuronavigation system. The aims of this study were to present our primary experiences with SEEG using SA and to compare the accuracy of implantation between SA and navigation-guided manual adjustment (MA). Seventeen electrodes from two patients who underwent SEEG with SA and 18 electrodes from four patients with MA were retrospectively reviewed. We measured the distance between the planned location and the actual location at entry (De) and the target (Dt) in each electrode. The length of the trajectory did not show a strong correlation with Dt in SA (Pearson's correlation coefficient [r] = 0.099, p = 0.706) or MA (r = 0.233, p = 0.351). De and Dt in SA were shorter than those in MA (1.99 ± 0.90 vs 4.29 ± 1.92 mm, p = 0.0002; 3.59 ± 2.22 vs 5.12 ± 1.40 mm, p = 0.0065, respectively). SA offered higher accuracy than MA both at entry and target. Surgical times per electrode were 38.9 and 32 min in the two patients with SA and ranged from 51.6 to 88.5 min in the four patients with MA. During the implantation period of 10.3 ± 3.6 days, no patients experienced any complications.**

Keywords: SEEG, epilepsy surgery, robot arm, neuronavigation, Autoguide

## Introduction

In the presurgical evaluation of epilepsy, long-term video electroencephalography (EEG) with intracranial electrode placement is performed when the epileptogenic zone cannot be identified with non-invasive evaluations such as scalp EEG, computed tomography (CT), magnetic resonance imaging (MRI), and positron emission tomography. Intracranial electrodes are classified as subdural electrodes and depth electrodes. Subdural electrodes are advantageous for detection of propagation of a seizure on the brain surface and for localization of brain functions by electrical cortical stimulation. However, subdural electrodes have several disadvantages. First, a large craniotomy must be made for the implantation. Second, epileptic activity in deep brain areas cannot be evaluated.[1] Depth electrodes can compensate for these shortcomings, and recently, the use of stereotactic electroencephalography (SEEG) with depth electrodes has become common in European countries as well as in the United States.[2-5]

To perform SEEG, the stereotactic method of electrode insertion is applied. Conventionally, SEEG is performed with a stereotactic frame designed for brain surgery.[6-8] In brief, after mounting the stereotactic frame on the patient's head, volumetric data of CT or MRI are obtained to co-register the patient's brain and the frame. Then, the trajectory is fixed with the frame. Through this trajectory, the skull and the dura are perforated, followed by puncturing

Received January 14, 2022; Accepted March 31, 2022

the brain and inserting the electrode. This stereotactic method is also applied for insertion of electrodes for deep brain stimulation, stereotactic hematoma removal, and needle biopsy. However, the number of punctures of the brain is at most two in these procedures. On the other hand, more electrodes (usually 7-14 electrodes) are implanted depending on the hypothesis in SEEG.[9] Thus, the setting of the trajectory of each electrode leads to a longer surgical time. Recently, a robotic arm for automatic adjustment of the trajectory was invented and is becoming more commonly used. Robot-assisted SEEG has contributed to the reduction of the surgical time and has a low complication rate and comparable accuracy.[10]

According to the Japanese health insurance system in 2020, the use of a robotic arm is recommended when more than seven electrodes are planned to be implanted. Currently, three types of robotic arms are commercially available in Japan. Among them, Stealth Autoguide (SA) (Medtronic, Minneapolis, MN, USA) functions as an optional instrument of the neuronavigation system. The clinical use of SA was approved by the Pharmaceuticals and Medical Devices Agency in Japan in February 2021. The number of SEEGs performed is increasing, along with increasing use of the robotic arm. However, no clinical reports have compared SA and navigation-guided manual adjustment (MA), which has been conventionally used for stereotactic brain biopsy. The aims of the present study were to present our primary experiences with SEEG using SA and to compare the accuracy of implantation between SA and MA.

## Materials and Methods

### Subjects

The present study is a retrospective multicenter design that was approved by the ethics committee of Osaka City University Hospital (IRB No. 2021-180). In total, six patients who underwent epilepsy surgery following depth electrode placement were enrolled. Among them, two patients (Pt 1, 2) underwent SEEG using SA in March 2021 and June 2021 in Osaka City University Hospital. To compare the accuracy of implantation, four patients (Pt 3-6) who underwent SEEG with MA in Osaka City University Hospital or Osaka City General Hospital between July 2020 and March 2021 were enrolled. Written informed consent was waived in the form of opt-out, and we announced the study and stated the opportunity for non-participation to subjects in Osaka City University Hospital. Written informed consent was obtained in Osaka City General Hospital. Depth electrodes in Pt 3-6 were implanted with the Vertek passive biopsy system (Medtronic).

### Planning of electrode implantation

For all patients, the locations of implantation were preoperatively planned using the neuronavigation system (Stealth station [Medtronic]). Three-dimensional T1-weighted MRI, CT angiography, and CT venography were superimposed. An entry was defined as the planned point of insertion on the brain surface. A target was defined as the planned tip of the electrode. The entries and targets were planned to not cross arteries, veins, and the lateral ventricle. If possible, the angle of the trajectory was planned to not exceed 30° from the perpendicular line of the skull, because a higher angle may contribute to deviation errors.[11] Distances from the target to the entry and the bone thickness on the trajectory were measured for each electrode (Fig. 1). Depth electrodes 1.5 mm in diameter and with 5-mm intervals between each of 6 or 10 contacts (Unique Medical, Tokyo, Japan) were used.

### Surgery

The patient's head was fixed with the three-pin Mayfield head holder. In Pt 1 and 2, the targeting unit of SA was fixed on the head holder or on the frame of the surgical bed (Fig. 2a). After briefly prepositioning the targeting unit close to the planned insertion trajectory, the precise trajectory was automatically adjusted (Fig. 2b). A 1-cm skin incision for each electrode was made. Drilling of a 3.2-mm diameter hole in the skull was performed with the Midas Rex Depth Stop tool (Medtronic) through the adjusted trajectory. The depth of the drilling was set at 1 mm plus the measured bone thickness (Fig. 2c). When the dura was not penetrated by the drilling, we penetrated the dura with monopolar electrical cautery.

In Pt 3-6, each trajectory and target were manually adjusted and locked under navigation guidance with the Vertek passive biopsy system (Medtronic). A 2-cm skin incision was made, and the skull was perforated with a 5-mm drill. The dura was penetrated with monopolar electrical cautery. In both methods, the brain was punctured with a passive biopsy needle (Medtronic) (Fig. 2d) or navigation-registered needle (Fig. 2e),[12] both of which were 2.1 mm in diameter. Punctures were processed while confirming the trajectory and the tip of the needle with the navigation system. After moving the tip to the target, we marked it on fluoroscopy. Thereafter, we removed the needle and inserted the depth electrode. We confirmed that the electrode tip was located on the target under fluoroscopy. In Pt 1, depth electrodes were fixed to the skull with a titanium plate and thread.[12,13] In Pt 2, the electrodes were fixed to the skin with threads (Fig. 2f).[14] These were temporary methods of fixation because the fixation bolt was not available in Japan at the time of surgery. In Pt 3-6, depth electrodes were fixed to the skull with threads using a small hole made on the skull edge.

### Evaluations

MRI in patients with implanted electrodes is prohibited in Japan. Thus, postoperative CT and preoperative MRI were superimposed with Stealth station and used for

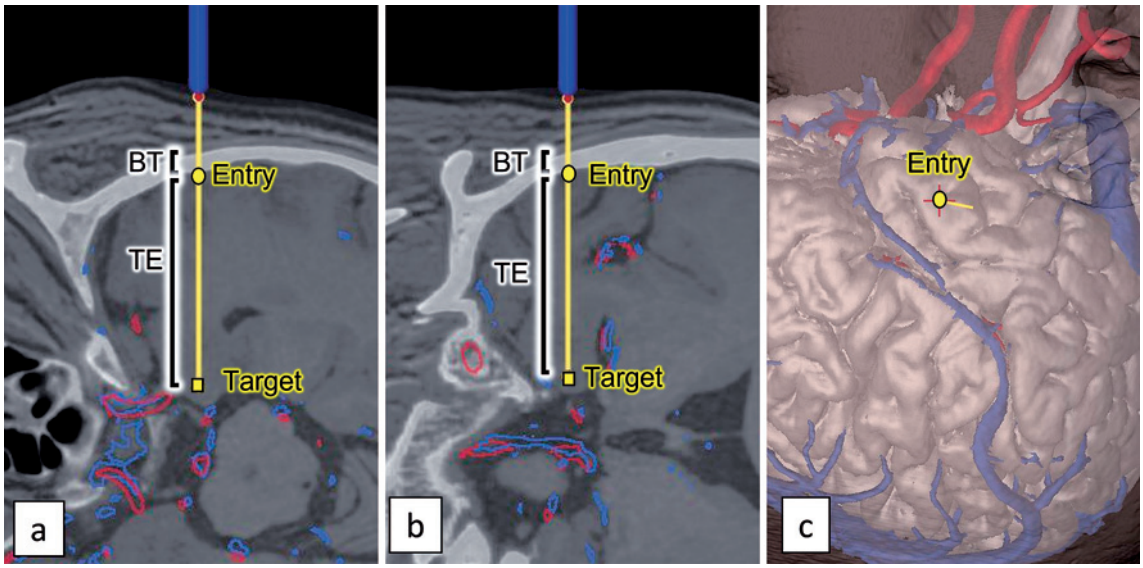


**Fig. 1 Planning of electrode implantation. An entry was defined as the planned point of insertion on the brain surface. A target was defined as the planned tip of the electrode. Distances from the target to the entry (TE) and the bone thickness (BT) on the trajectory were measured. (a, b) Trajectory view, (c) three-dimensional view.**

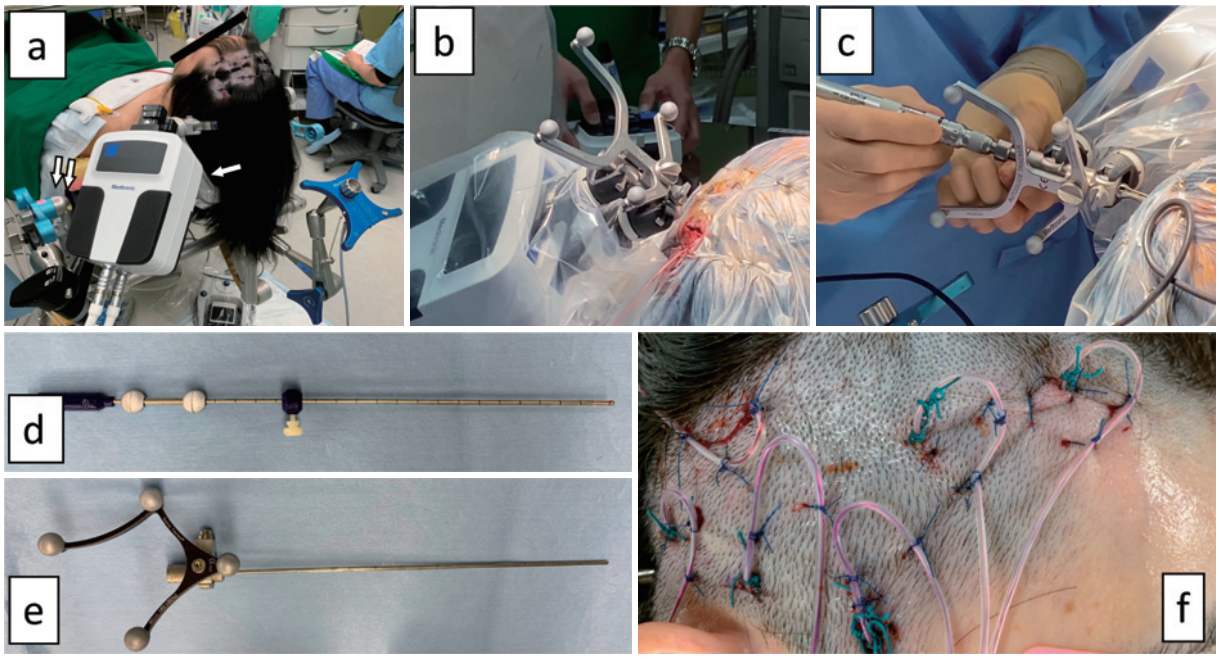


**Fig. 2 Surgical steps of electrode implantation.**
**(a) Targeting unit of the Stealth Autoguide (white arrow) was fixed on the frame of the surgical bed (white double arrow).**
**(b) After briefly prepositioning the targeting unit close to the planned trajectory, the precise trajectory was automatically adjusted.**
**(c) Drilling of a 3.2-mm diameter hole in the skull was performed through the adjusted trajectory.**
**(d) Passive biopsy needle for brain puncture.**
**(e) Navigation-registered needle for brain puncture.**
**(f) Fixation of the electrodes to the skin with threads.**

evaluation of accuracy. We compared the location of the preoperative planning and implanted electrode for each electrode. The distances between the planned entry and the actual insertion point of the implanted electrode were measured in the coronal (X mm), sagittal (Y mm), and axial (Z mm) sections. Additionally, the distances between

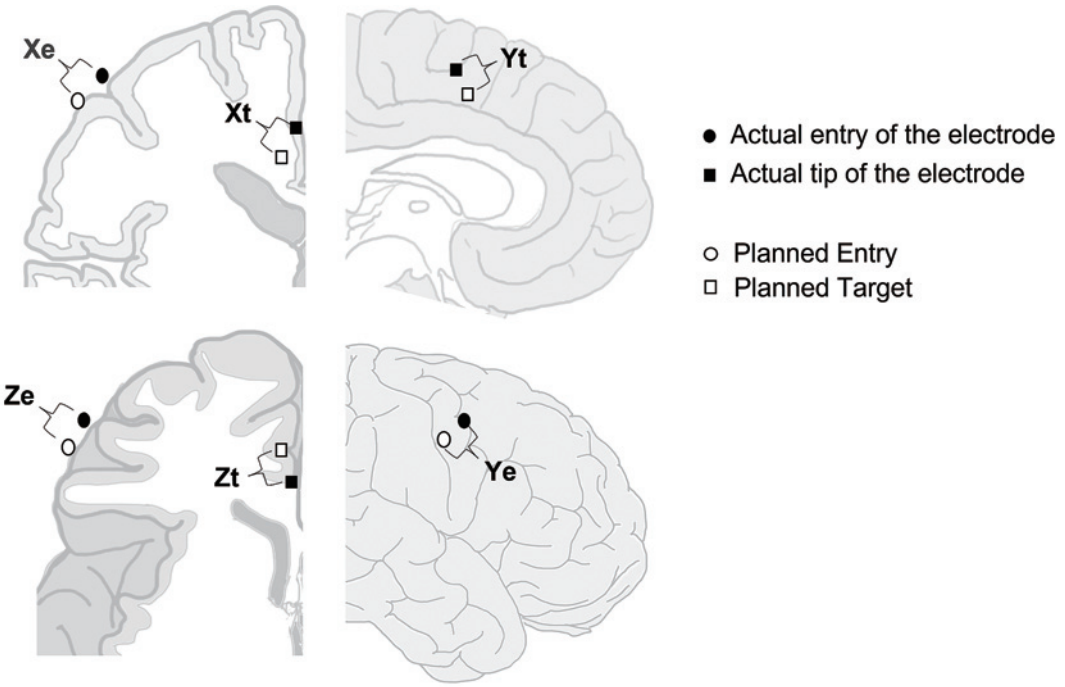


**Fig. 3 Measurement of the differences of the planned point and actual implanted point of the electrode. The distances between the planned entry and the actual implanted point of the electrode were measured in the coronal (X mm), sagittal (Y mm), and axial (Z mm) sections (Xe, Ye, Ze). Additionally, the distances between the planned target and the actual tip of the implanted electrode were measured in the three sections (Xt, Yt, Zt).**

the planned target and the actual tip of the implanted electrode were measured in the three sections (Fig. 3). Then, the difference of the entry (De) and that of the target (Dt) were calculated with the following formulas:

$De = \sqrt{Xe^2 + Ye^2 + Ze^2}$ and $Dt = \sqrt{Xt^2 + Yt^2 + Zt^2}$.

First, the relationships between the length of trajectory and Dt were evaluated in SA and MA with Pearson's product-moment correlation coefficient (r). Second, De and Dt were compared between SA and MA with the Wilcoxon signed-rank test.

Surgical times per electrode and perioperative complications such as hemorrhage and ischemia, cerebrospinal fluid leakage, and surgical site infection were reviewed. A p-value <0.05 was regarded as a significant difference.

## Results

### Summary of the patients and depth electrode placement

In Pt 1, the epileptogenic zone was mainly suspected to be in the left frontal lobe, but the possibility of her seizures originating from the right frontal lobe could not be excluded (Table 1). In total, eight electrodes were implanted in the bilateral frontal lobes. In Pt 2, the epileptogenic zone was suspected to be in the bilateral temporal lobes and right frontal lobe. In total, nine electrodes were implanted in the bilateral temporal and frontal lobes. In Pt 3-6, four, two, seven, and five electrodes were implanted, respectively, depending on the suspected epileptogenic zones. After evaluations with depth electrode implantation, the suspected epileptogenic zone was resected in each patient.

### Correlation between the length of trajectory and Dt

The relationships between the length of trajectory and Dt were demonstrated with a scatter plot (Fig. 4) in SA and MA. In both methods, Pearson's correlation coefficients were low (r = 0.099 and 0.233, respectively), and corresponding p values for these correlations were not significant (p = 0.706 and 0.351, respectively).

### Accuracy of implantation with Autoguide compared with MA

During the implantation surgery, we did not encounter a large amount of cerebrospinal fluid leakage from the burr hole. For the 17 electrodes implanted with SA, De was 1.99 ± 0.90 mm (mean ± standard deviation [SD]), and Dt was 3.59 ± 2.22 mm (mean ± SD). For the 18 electrodes implanted with MA, De was 4.29 ± 1.92 mm (mean ± SD), and Dt was 5.12 ± 1.40 mm (mean ± SD). Both De and Dt in SA were shorter than those in MA (p = 0.0002 and 0.0065, respectively) (Fig. 5).

### Surgical time and perioperative complications

Surgical times per electrode with SA were 38.9 min in Pt 1 and 32 min in Pt 2. Surgical times per electrode with

**Table 1 Patient characteristics**

| Patient no. | Age (year) | Sex | Etiology | Method of stereotaxy | No. of electrodes | No. of contacts | Side | Entry | Target | Length of trajectory (mm) | Surgical time (min) | Surgical time/no. of electrodes (min) | De (mm) | Dt (mm) | Period of electrode implantation (day) | Surgery |
|---|---|---|---|---|---|---|---|---|---|---|---|---|---|---|---|---|
| 1 | 29 | F | Unknown | Auto guide | 8 | 6 | L | Post. SFG | SMA | 28.7 | 311 | 38.9 | 1.88 | 2.45 | 8 | Lt frontal gyrectomy |
| | | | | | | 10 | L | Post. SFG | Mid. cingulate | 37.7 | | | 2.17 | 7.21 | | |
| | | | | | | 10 | L | Ant. SFG | Frontal base | 54.3 | | | 2.49 | 1.53 | | |
| | | | | | | 10 | L | Ant. MFG | Ant. cingulate | 46.2 | | | 1.92 | 1.71 | | |
| | | | | | | 10 | L | Post. MFG | Mid. cingulate | 48.4 | | | 0.67 | 2.89 | | |
| | | | | | | 6 | L | Ant. MTG | Ant. phg | 45.9 | | | 1.86 | 5.47 | | |
| | | | | | | 6 | R | Ant. SFG | Ant. cingulate | 37.4 | | | 0.54 | 2.58 | | |
| | | | | | | 10 | R | Ant. MFG | Frontal pole | 53 | | | 2.65 | 2.71 | | |
| 2 | 51 | F | Encephalitis | Auto guide | 9 | 10 | R | Ant. MTG | Amygdala | 44.1 | 288 | 32 | 1.98 | 3.65 | 15 | Rt frontal disconnection |
| | | | | | | 10 | R | Ant. MTG | Ant. phg | 45.6 | | | 0.71 | 9.58 | | |
| | | | | | | 10 | R | Post. MTG | Post. phg | 43.2 | | | 0.9 | 3.78 | | |
| | | | | | | 6 | R | Ant. MFG | – | 28 | | | 1.58 | 1.97 | | |
| | | | | | | 6 | R | Post. IFG | – | 25.1 | | | 1.98 | 2.05 | | |
| | | | | | | 10 | L | Ant. MTG | Amygdala | 42.2 | | | 3.15 | 2.31 | | |
| | | | | | | 10 | L | Ant. MTG | Ant. phg | 43.3 | | | 2.7 | 1.57 | | |
| | | | | | | 10 | L | Post. MTG | Post. phg | 43.4 | | | 3.17 | 5.7 | | |
| | | | | | | 6 | L | Post. IFG | – | 27.1 | | | 3.47 | 3.83 | | |
| 3 | 37 | F | Hippocampal sclerosis | Vertek biopsy | 4 | 6 | L | Occipital lobe | Phg | 59 | 354 | 88.5 | 5.02 | 5.6 | 8 | Rt. SAH |
| | | | | | | 6 | R | Occipital lobe | Phg | 63 | | | 4.87 | 4.46 | | |
| | | | | | | 6 | R | Ant. SFG | Ant. insula | 81.8 | | | 6.12 | 6.81 | | |
| | | | | | | 6 | R | Ant. SFG | Frontal base | 90 | | | 4.33 | 8.08 | | |
| 4 | 19 | F | Hippocampal sclerosis | Vertek biopsy | 2 | 6 | L | Occipital lobe | Phg | 72.1 | 155 | 77.5 | 4.39 | 6.27 | 8 | Rt. SAH |
| | | | | | | 6 | R | Occipital lobe | Phg | 66.3 | | | 2.62 | 2.6 | | |
| 5 | 59 | F | Unknown | Vertek biopsy | 7 | 10 | L | Post. MFG | Mid. cingulate | 54.8 | 361 | 51.6 | 0.92 | 5.58 | 15 | Lt. frontal gyrectomy |
| | | | | | | 6 | L | SPL | Post. insula | 86.5 | | | 1.56 | 3.68 | | |
| | | | | | | 10 | L | Ant. MTG | Ang. phg | 45.4 | | | 4 | 5 | | |
| | | | | | | 6 | L | Ant. MFG | Ant. cingulate | 45 | | | 8.35 | 3.61 | | |
| | | | | | | 6 | L | Ant. MFG | Frontal base | 41.4 | | | 4.71 | 4.71 | | |
| | | | | | | 10 | L | Post. MTG | Post. phg | 42.7 | | | 2.67 | 4.69 | | |
| | | | | | | 10 | L | Ant. MTG | Amygdala | 42 | | | 3.95 | 3.37 | | |
| 6 | 10 | M | Unknown | Vertek biopsy | 5 | 6 | R | Ant. MTG | Ant. phg | 41 | 319 | 63.8 | 5.23 | 6.6 | 8 | Rt. TL |
| | | | | | | 6 | R | Ant. MTG | Temporal tip | 41.1 | | | 3.48 | 5.97 | | |
| | | | | | | 6 | R | Post. MTG | Temporal base | 23 | | | 2.48 | 5.85 | | |
| | | | | | | 6 | R | Ant. MTG | Amygdala | 31.2 | | | 7.78 | 5.47 | | |
| | | | | | | 6 | R | Post. ITG | Temporal base | 29.7 | | | 4.74 | 3.81 | | |

SFG: superior frontal gyrus; MFG: middle frontal gyrus; MTG: middle temporal gyrus; IFG: inferior frontal gyrus; SPL: superior parietal lobule; ITG: inferior temporal gyrus; SMA: supplementary motor area; Phg: parahippocampal gyrus; SAH: selective amygdalohippocampectomy; TL: temporal lobectomy

MA were 88.5, 77.5, 51.6, and 63.8 min in Pt 3-6, respectively. During the implantation period of 10.3 ± 3.6 days (mean ± SD), no patients experienced hemorrhagic and ischemic complications, cerebrospinal fluid leakage, or surgical site infection.

## Discussion

### Summary of the results

We demonstrated that the length of the trajectory did not show a strong correlation with Dt in SA and MA, and

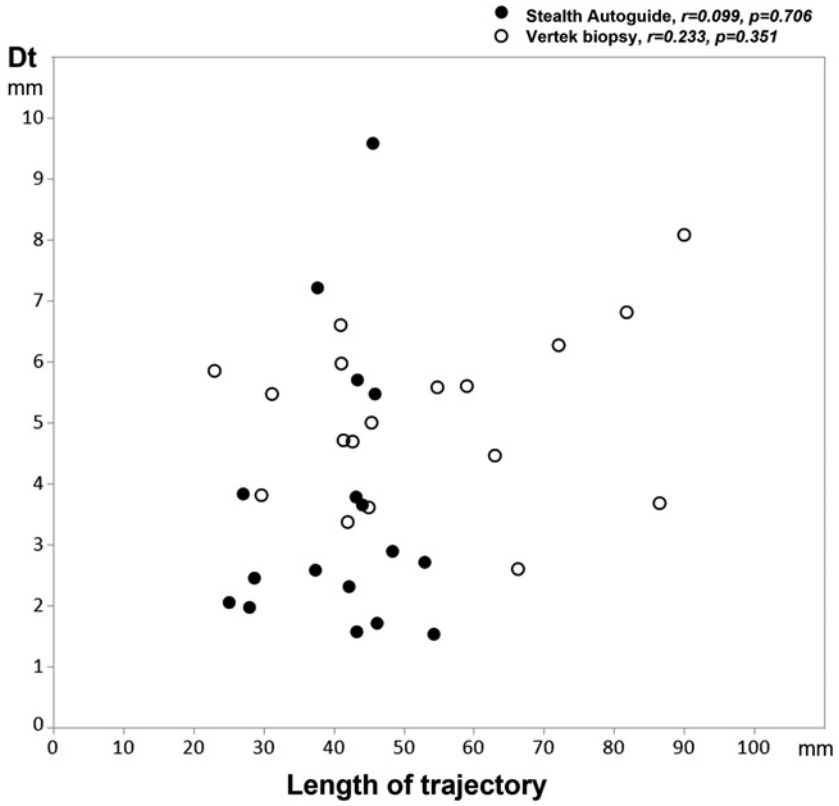


**Fig. 4 The relationships between the length of trajectory and Dt were demonstrated in SA (Pt 1 and 2) and MA (Pt 3–6). In both methods, Pearson's correlation coefficients were low (r = 0.099 and 0.233, respectively), and corresponding p values for these correlations were not significant (p = 0.706 and 0.351, respectively).**

that the distance between the planned and implanted electrode with SA was shorter than that with MA, suggesting that SA offers better accuracy of implantation than MA.

The surgical time per electrode may be shorter in SA than in MA. However, because of the small number of patients, we did not compare the times statistically. Additionally, we did not compare surgical complications such as hemorrhage, ischemia, and surgical site infection because of the small number of patients. We excluded seizure outcomes following surgery from the comparison because the outcome is not considered to be related to the method of implantation. To the best of our knowledge, the present study is the first comparative study between SA and MA in the clinical setting.

**Robotic arms**

Currently, several robot-assisted stereotactic systems are available. Globally, floor-based robotic arms such as ROSA (Zimmer Biomet, Warsaw, IN, USA) and Neuromate (Renishaw, New Mills, UK) are commonly used for SEEG. Recently, two robotic arms that work as optional instruments with the neuronavigation system were launched (SA and Cirq [BrainLab AG, Feldkirchen, Germany]). Compared with floor-based robotic arms, these instruments appear to provide less, but sufficient, flexibility for adjustment of the planned trajectory. These instruments are used by fixing them on the head holder or the surgical bed, enabling surgeons to change the height and angle of the surgical bed during the operation.[15] Currently, most epilepsy centers in Japan have a neuronavigation system but do not have a robotic arm for SEEG. In such a situation, robotic arms with optional instruments for the navigation system will play an important role in introducing SEEG to Japan with respect to the initial cost of the investment.

**SA**

SA is a miniature-designed and easy-handling robotic system for stereotactic interventions, which was originally invented as iSYS1.[15,16] The targeting unit of SA consists of two flat modules that can move against one another, and it allows precise angulation (±30°) and translational positioning (±20 mm) of the instrument guidance sheath with submillimeter precision. According to previous reports, iSYS1 offers higher accuracy than MA in a preclinical cadaveric study[15] and 3D-printed skull phantom.[16,17] Another preclinical study with a cadaveric brain demonstrated that SA offers comparable accuracy compared with frame-based procedures.[18]

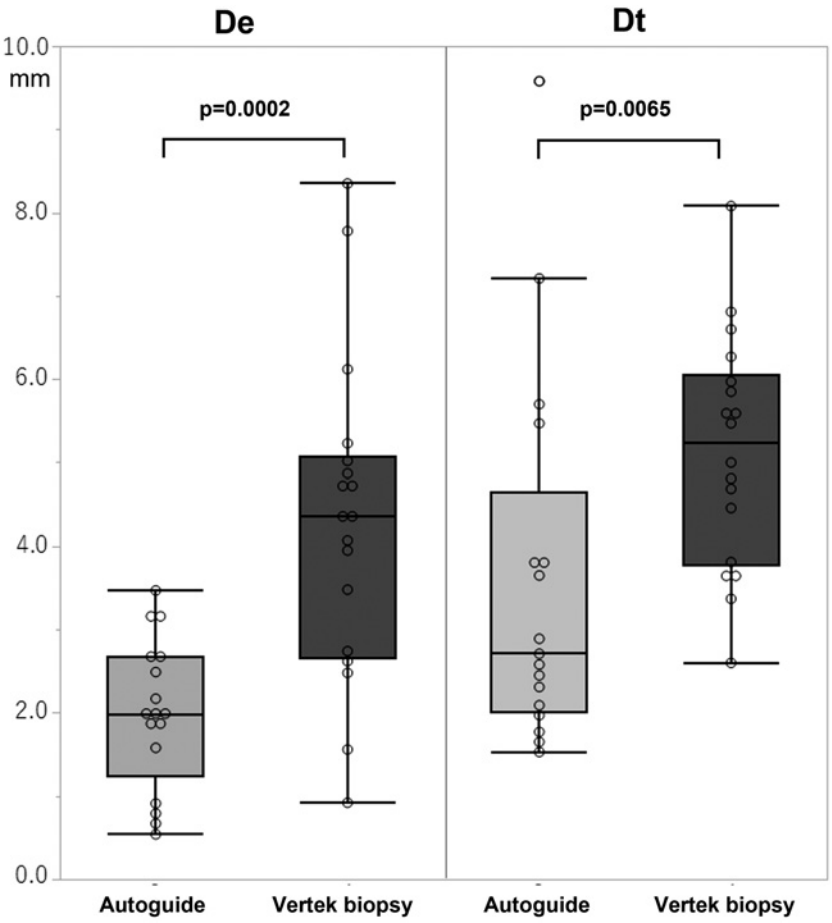


**Fig. 5 Comparison of the distance between the entry and the target in Stealth Autoguide and manual adjustment with Vertek passive biopsy. De was 1.99 ± 0.90 mm, and Dt was 3.59 ± 2.22 mm with Stealth Autoguide (mean ± SD). De was 4.29 ± 1.92 mm, and Dt was 5.12 ± 1.40 mm with manual adjustment (mean ± SD). Both De and Dt in SA were shorter than those in MA (p = 0.0002 and 0.0065, respectively).**

**Accuracy of the implantation**

According to a systematic review and meta-analysis, the mean error of the entry point was 1.17 mm (95% confidence interval, 0.80-1.53), and the mean error of the target point was 1.71 mm (95% confidence interval, 1.66-1.75) in robotic trajectory guidance systems.[19] In our results, the mean error of the entry in SA was 1.99 ± 0.90 mm (mean ± SD), which appears comparable with the meta-analysis because of the submillimeter difference. On the other hand, the target error (3.59 ± 2.22 mm [mean ± SD]) in our results was larger than that in the meta-analysis. This difference may be due to the following two reasons. First, the entry point and the trajectory of insertion were adjusted by the robotic arm, whereas the depth of the tip was not adjusted automatically and manually determined with navigation guidance and fluoroscopy. Second, we were not able to use the bolt to fix the electrode to the skull at the time of surgery. After the fixation bolt becomes available in Japan, the accuracy of the target point is expected to be higher. Both entry error and target error in MA were larger than those in SA, which suggested a limitation of MA.

**Surgical tips in neuronavigation-based SEEG**

In neuronavigation-guided frameless SEEG, registration errors that directly influence the accuracy of implantation should be considered. These errors are derived from imaging distortion and the method used for intraoperative registration. Considering that these registration errors are at most 2 mm, planning should be made to not cross arteries and veins, especially veins on the brain surface. In addition, during implantation, unintentional deviations of the reference arc of the neuronavigation system or the head holder inevitably lead to vital registration errors. Surgeons must pay maximum attention to avoid this kind of arbitrary error.

**Limitations of the study**

The first limitation of the present study is the small number of patients. If we are able to collect more patients

who underwent SEEG with SA and MA, the surgical time in SA may be significantly shorter than that in MA. However, the number of patients who undergo SEEG with MA cannot be increased after introduction of SA because the accuracy of implantation is much higher with SA. Second, the comparison of SA and frame-based SEEG is also of interest for demonstrating the usefulness of SA. However, because the Japanese health insurance system recommends the use of the robotic arm for SEEG, creating a prospective study design at the single institutional level is difficult. A multicenter study that includes centers still conducting frame-based SEEG is warranted for comparing robot-assisted frameless and frame-based SEEG. Third, we did not evaluate the trajectory angle, which may affect the accuracy of implantation. Finally, the method of electrode implantation described in the present study is likely to change because the fixation bolt and thin-sized electrodes (0.8 mm in diameter) are not yet available in Japan.

## Conclusions

Compared with neuronavigation-guided MA, depth electrode implantation with SA offered significantly higher accuracy in SEEG. Additionally, the use of SA may contribute to a shorter surgical time.

## Abbreviation List

CT: computed tomography, EEG: electroencephalography, MA: manual adjustment, MRI: magnetic resonance imaging, SA: Stealth Autoguide, SEEG: stereotactic electroencephalography

## Conflicts of Interest Disclosure

All authors have no conflicts of interest. All Japan Neurosurgical Society member authors have registered online Self-reported COI Disclosure Statement Forms through the website.

## References

1) George DD, Ojemann SG, Drees C, Thompson JA: Stimulation mapping using stereoelectroencephalography: current and future directions. *Front Neurol* 11: 320, 2020
2) Abou-Al-Shaar H, Brock AA, Kundu B, Englot DJ, Rolston JD: Increased nationwide use of stereoencephalography for intracranial epilepsy electroencephalography recordings. *J Clin Neurosci* 53: 132-134, 2018
3) Iida K, Otsubo H: Stereoelectroencephalography: indication and efficacy. *Neurol Med Chir (Tokyo)* 57: 375-385, 2017
4) Yamamoto T: Recent advancement of technologies and the transition to new concepts in epilepsy surgery. *Neurol Med Chir (Tokyo)* 60: 581-593, 2020
5) Fiani B, Jarrah R, Doan T, Shields J, Houston R, Sarno E: Stereoelectroencephalography versus subdural electrode implantation to determine whether patients with drug-resistant epilepsy are candidates for epilepsy surgery. *Neurol Med Chir (Tokyo)* 61: 347-355, 2021
6) Gonzalez-Martinez J, Mullin J, Vadera S, et al.: Stereotactic placement of depth electrodes in medically intractable epilepsy. *J Neurosurg* 120: 639-644, 2014
7) Cardinale F, Cossu M, Castana L, et al.: Stereoelectroencephalography: surgical methodology, safety, and stereotactic application accuracy in 500 procedures. *Neurosurgery* 72: 353-366; discussion 366, 2013
8) Bancaud J, Angelergues R, Bernouilli C, et al.: Functional stereotaxic exploration (SEEG) of epilepsy. *Electroencephalogr Clin Neurophysiol* 28: 85-86, 1970
9) Isnard J, Taussig D, Bartolomei F, et al.: French guidelines on stereoelectroencephalography (SEEG). *Neurophysiol Clin* 48: 5-13, 2018
10) González-Martínez J, Bulacio J, Thompson S, et al.: Technique, results, and complications related to robot-assisted stereoelectroencephalography. *Neurosurgery* 78: 169-180, 2016
11) Iordanou JC, Camara D, Ghatan S, Panov F: Approach angle affects accuracy in robotic stereoelectroencephalography lead placement. *World Neurosurg* 128: e322-e328, 2019
12) Fujimoto A, Masuda Y, Ichikawa N, et al.: Side slit guide pipe for precise placement of depth electrodes. *World Neurosurg* 126: 291-295, 2019
13) Fujimoto A, Sakakura K, Ichikawa N, Okanishi T: Easy anchoring and smaller skin incision procedure for neuronavigation-based frameless stereoelectroencephalography. *J Clin Neurosci* 74: 220-224, 2020
14) Khoo HM, Hall JA, Dubeau F, et al.: Technical aspects of SEEG and its interpretation in the delineation of the epileptogenic zone. *Neurol Med Chir (Tokyo)* 60: 565-580, 2020
15) Minchev G, Kronreif G, Martinez-Moreno M, et al.: A novel miniature robotic guidance device for stereotactic neurosurgical interventions: preliminary experience with the iSYS1 robot. *J Neurosurg* 126: 985-996, 2017
16) Dorfer C, Minchev G, Czech T, et al.: A novel miniature robotic device for frameless implantation of depth electrodes in refractory epilepsy. *J Neurosurg* 126: 1622-1628, 2017
17) Vakharia VN, Rodionov R, McEvoy AW, et al.: Improving patient safety during introduction of novel medical devices through cumulative summation analysis. *J Neurosurg* 130: 213-219, 2018
18) Brandman D, Hong M, Clarke DB: Preclinical evaluation of the Stealth Autoguide robotic guidance device for stereotactic cranial surgery: a human cadaveric study. *Stereotact Funct Neurosurg* 1-8, 2021
19) Vakharia VN, Sparks R, O'Keeffe AG, et al.: Accuracy of intracranial electrode placement for stereoencephalography: a systematic review and meta-analysis. *Epilepsia* 58: 921-932, 2017

Corresponding author: Takehiro Uda, MD, PhD.
Department of Neurosurgery, Osaka Metropolitan University Graduate School of Medicine, 1-4-3 Asahi-machi, Abeno-ku, Osaka, 545-8585, Japan.
*e-mail*: udat@omu.ac.jp